E3S Web of Conferences **415**, 03022 (2023) https://doi.org/10.1051/e3sconf/202341503022
DFHM8

Landslide Analysis combining Laser Scanning and Photogrammetry

Pedro Pinto*[1], *Juliana* Barros[2], *Marisa* Pinheiro[2]***, *Roberto* Tomás[3], *Tiago* Miranda, and *Eduardo* Pereira[1]**

[1]ISISE, University of Minho, 4800-058 Guimaraes, Portugal
[2]Level, a Geotechnical Management Company, 4700-727 Braga, Portugal
[3]Civil Engineering Department, University of Alicante, Spain.

Abstract. After a sequence of weeks of heavy raining, a catastrophic mass movement occurred in the parish of Palmeira de Faro, Esposende (N Portugal) on November 23, 2022. The collapsed slope presented a maximum height of about 21 m and a length of 45 m. In order to document and analyse this case from the geotechnical perspective, a general survey was devised including the use of aerial photography, laser scanning and conventional topographic survey methods. The results obtained showed that these techniques provide very accurate and abundant information that is essential to support a comprehensive documentation of the features and variables of the slope. The mechanisms involved in this catastrophic collapse are still under investigation, and causes such as the excessive rainfall in the previous months or geologic conditions are still being considered, although currently the existing information seems to indicate for a combination of debris flow / rock slide driven event.

1 Introduction

Nowadays there seems to exist an increasing trend for the occurrence of unexpected mass movements and extreme weather events, very likely related to climate changes. The possibilities of current technologies are particularly interesting in this context. Photography has been used for quite some time as a source of data for mapping and interpreting landforms, and the extraction of quantitative elevation information from stereophotography, under the umbrella term of photogrammetry [1, 2]. Also, spurred by developments in traditional ground surveying, such as the advent of differential GNSS and reflectorless, robotic total stations, the acquisition of topographic data has been transformed most significantly by a new generation of remote sensing technologies, that have transformed the digital elevation modelling and geomorphological terrain analysis [3]. For instance, terrestrial laser scanning [4] and automated digital photogrammetry [2, 5] in particular, have revolutionized the quality of digital elevation models (DEMs), extending their spatial extent, resolution, and accuracy [3]. Moreover, since its emergence, automated aerial and close-range digital photogrammetry has become a powerful and widely used tool for three-dimensional topographic modelling [3], that can be acquired from a range of cheap, lightweight platforms on which imaging sensors are deployed such as drones [6].

The slope under the study was located in the north region of Portugal, in the Parish of Esposende (fig. 1). According to Geological Chart of Portugal with scale 1:50000 – sheet 5-C (Barcelos) is composed essentially by a monzonitic granite predominantly biotitic, with porphyroid texture and medium grain, sometimes coarse [7]. As discussed in a previous publication [8], this slope suffered a catastrophic landslide after a particularly rainy autumn, and caused two casualties. The site is complex, with strong slope discontinuities, vegetation, trees and the presence of houses and other infrastructures.

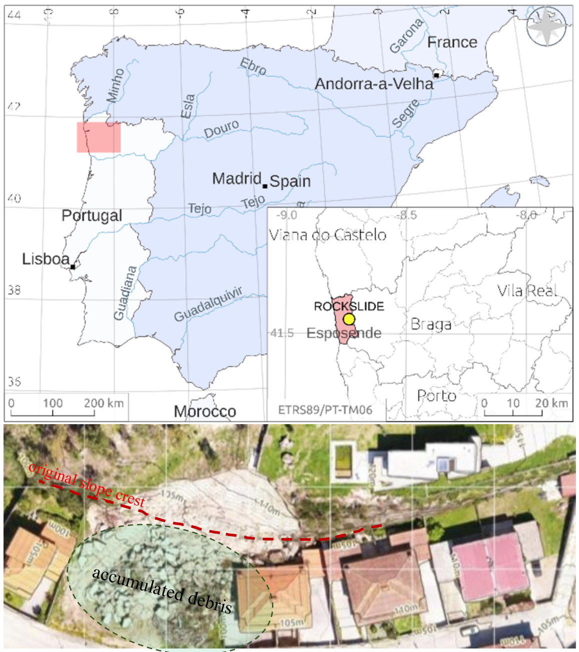

Fig. 1. Rockslide location, in Palmeira de Faro, Esposende, and orthomosaic showing the original slope crest, the sliding plane, and the area where the debris accumulated.

* Corresponding authors: id10434@alunos.uminho.pt;
** eduardo.pereira@civil.uminho.pt;
*** marisapinheiro@level-gam.com

2 Methodology

Considering that the slope was mostly a heavily weathered granitic rock mass, with visible fracturing and residual soil involving large blocks, besides the geometrical information it was important to document the orientation of the discontinuity families in the distinct parts of the cut slope. Initially, the intention was to use photogrammetry to obtain the overall geometric representation, not only of the sled slope but also of the adjacent cut slopes that remained intact, as well as the surroundings. Laser scanning was adopted with the aim of obtaining a high-resolution representation of the discontinuities visible at the surface of the cut slopes that remained intact, which apparently were less weathered.

2.1 Photogrammetry

The photogrammetric survey was performed using a DJI drone (Inspire 2) equipped with a 20 Mpix resolution camera (DJI MFT 15 mm, F1.7, 3.28 µm), and a GNSS rover receiver (Unistrong, G970-II) in RTK phase difference mode, with a reference station approximately 30 km away (Braga). The flight plan was set to ensure 70% and 80% of lateral and longitudinal photography overlap, respectively, 55 m maximum height above ground, a coverage area of 4.90 ac, and pixel resolution of 1.25 cm (fig.2). For calibration of the radial and tangential image distortion of the sensor, and georeferencing, eight ground control points (GCPs) were used (fig.2 b)), as a fundamental step to determine the quality of the DEM in the absolute reference frame [6].

Regarding the 3D terrain model generation, a proprietary software (Metashape® Professional - version 1.84), was used for dense cloud construction with 2D images. The resulting 3D model was then used for integrated geotechnical analysis of the terrain geometry, including the extraction of topographic heights and other features such as slopes and their orientations. For this purpose two open-source tools were used, QGIS® and CloudCompare®.

2.2 Laser Scanning

The laser survey was carried out using the Faro Focus 350 Laser Scanner series equipment. In order to survey the rocky slope, 8 sweeps were carried out. These scans were distributed in order to guarantee the partial overlapping of the scans and allow the subsequent seamless stitching of all scans in a unique bundle. As expectable, the higher the overlapping the lower the scanning error. The scans were then processed using FARO® SCENE software. After aggregating the various scans and cleaning up all the "noise" captured around the rocky slope, the point cloud was generated. Afterwards, CloudCompare ® and Revit ® were used to perform all the subsequent analyses, including cloud measurements and the automatic identification of discontinuities, which was one of the goals of this study.

3 Results

3.1 Photogrammetry

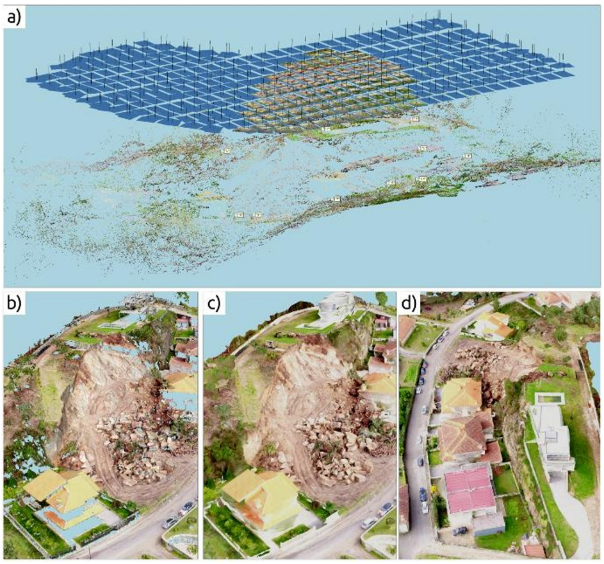

Fig. 2. Bundle adjustment of photo positions and alignment, after point-matching, for cloud densification and georeferencing using all pixels of the 372 images (sparse cloud in view, for clarity) a); colorized dense cloud with approximately 94 million points b); photo texturized 3D model in Northeast-Southwest c), and West-East d) viewing angles, not to scale.

Based on the GCPs and two validation points (VPs) surveyed with a GNSS receiver, it was possible to obtain a root mean square error (RMSE) of 4.19 cm (XY: 3.87 cm, Z: 1.61 cm) for the GCPs and 10.77 cm ((XY: 2.71 cm, Z: 10.42 cm) for the VPs. Since both RMSEs obtained for XY (horizontal plane) were similar, and considering that VPs were placed in unfavourable locations (too close to vertical walls and subject to higher error due to light reflectance and increased neighbour ground pixel saturation) and do not represent the overall sliding area, it was admissible to consider an overall uncertainty of ± 5 cm. Using Metashape® processing workflow, it was possible to retrieve the DEM (fig.3 a)) and the ortho-rectified mosaic (fig.2 b)), which were later exported to QGIS for contour, slope, and aspect extraction (fig.3 a), c-d)). Based on the results obtained it was possible to confirm that the topographic height of the sliding plane varied between 97 m and 118 m, the dip varied between 35º and 40º, and the aspect set towards SSW direction, at approximately 190º of azimuth.

3.2 Laser Scanning

The aggregated point cloud showed an average error of 13.8 mm, and the maximum error was somewhat higher, approximately 35 mm, and occurred between the scans in the extremities of the surveyed area. It should be noted that, for safety reasons and some limitations of the *in-situ* conditions, it was not always possible to position the equipment in the most favourable locations. The model obtained is shown in Fig.4.

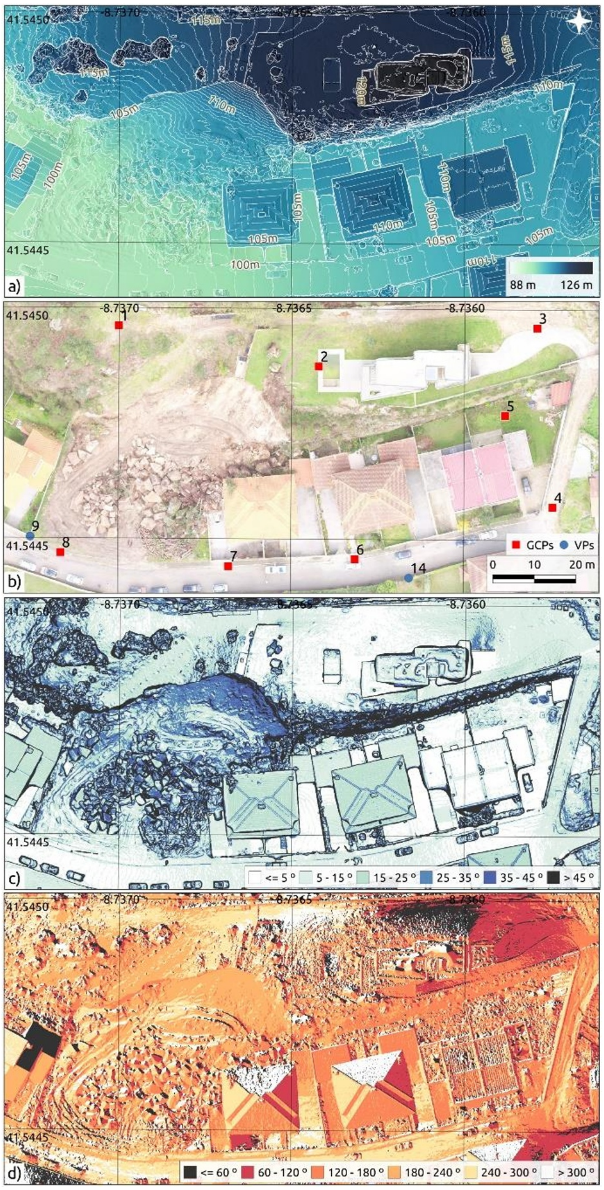

Fig. 3. Digital elevation model (DEM) with a spatial resolution of 5 cm/pixel, and ± 5 cm of uncertainty, with contour lines at 0.50 m spacing a); ortho-rectified photo mosaic based on DEM and cartographic projection ETRS89/PT-TM06, where X+ at East, Y+ at North and Z+ the height above mean sea level, with ground control points (GCPs) and validation points (VPs) for reference b); terrain slope c) and aspect d).

The point cloud obtained by laser scanning was subsequently used to automatically identify the discontinuity sets of the slope, in order to help understanding the possible causes of the landslide incident.

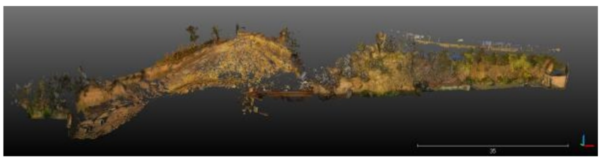

Fig. 4. 3D visualization of the coloured point cloud obtained by laser scanning on CloudCompare (x – red, y – green, z – blue) on CloudCompare®.

Therefore, the point cloud was cleaned using CloudCompare®, and a Matlab routine designated Discontinuities Set Extractor (DSE) was used to perform the identification [8]. As a result, a 3D visualization of the rock slope with the discontinuity sets identified was obtained (fig. 5a)), as well as their pole density in stereographic representation (fig. 5b). Table 1 presents the values of dip and dip direction of the principal poles (selected according to the major representative) – (J1 to J4).

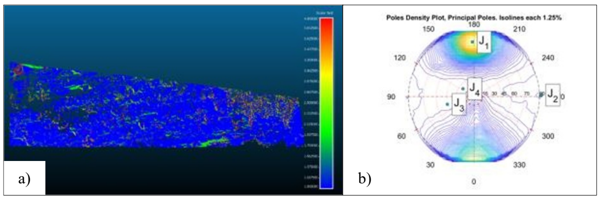

Fig. 5. Automatic identification of discontinuities: a) 3D visualization of rock slope with Cloud Compare®, with the planes of discontinuities identified using DSE routine; b) stereographic representation of principal discontinuities poles (J1, J2, J3 e J4).

Table 1. Most representative discontinuities poles are presented using dip and dip direction values and respective colors as identified in fig. 5a.

Discontinuities set	Dip (º)	Dip Direction (º)	Color of each set
J1	78	179	Blue
J2	38	350	Green
J3	67	60	Yellow
J4	65	288	Red

3.3 Combined analysis

Fig.6 shows the statistical analysis of the monthly rainfall time series. The results show that, after a long period of severe draught, two months of exceptional rainfall have preceded the catastrophic event. Therefore, precipitation has very likely influenced the mass movement observed. The visual inspection of the site has revealed that large blocks and soil in large amounts were forming the moved mass. Although the accident seems to show characteristics of both debris/landslide and rock movement, the final causes are still under investigation. The results allowed, in general, to distinguish the most favourable characteristics and weaknesses of both techniques used in the present case study. Regarding the photogrammetry approach using the drone, limitations were related to the use of passive sensors that depend on lighting and weather conditions, as well as sensor spatial, spectral, and radiometric resolution. The number and quality of ground control points also influence the quality of results, since the accuracy of the positioning system of the drone is typically insufficient to attain the best results. However, drone-based photogrammetry presents several advantages, such as the great cost-effectiveness, the possibility to access difficult or high-risk areas, fast results, high spatial and temporal resolutions, high accuracy scale, aerial view, automated data collection, open-source software availability and easiness of use.

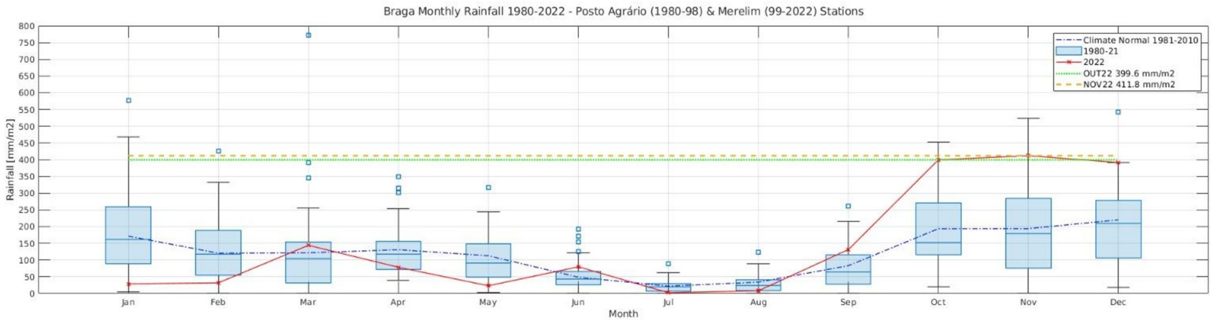

Fig. 6. Monthly rainfall statistics in the region since 1980.

In this particular case study, due to the presence of numerous terrain obstacles such as houses, walls, and vegetation, these advantages were essential to allow the production of an overall high-resolution model of the area, very useful to extract the slope features already identified.

Conversely, the effectiveness of ground-based laser scanning was limited by the ground obstacles that often didn't allow to position of the scanner in the optimal locations, leading to the creation of shadow areas and resulting in less-than-optimal beam orientations with respect to the scanned area. However, excluding extreme conditions, the laser scanner showed to be less sensitive to light and weather conditions, delivering more consistent results. Due to this, laser scanning results of the slope cut were the ones selected for the automatic identification of the discontinuities.

4 Discussion and conclusions

The combined interpretation of the results obtained allowed to understand that the orientation of the discontinuity sets with respect to the orientation of the slope cut was highly unfavourable, and very likely related to the landslide occurred. The photogrammetry results clearly helped to identify the formation of an almost perfectly flat sliding surface at the top part of the slope, which was determining the sliding kinematics. The dip and orientation of this flat surface perfectly matched the dip and dip orientation identified in the stereographic representation of the discontinuity sets, obtained by automatic identification using the laser scanning results. Therefore, the combined use of both techniques showed to be particularly advantageous in the description and analysis of the landslide that occurred. The analysis of the monthly rainfall time series also showed that exceptional rainfall preceded by a long period of severe draught may also have caused the observed mass movement. Therefore, a mix of debris flow and rockslide may be considered as well, as one form to describe the instability observed.

The use of multiple sensors and platforms to acquire and measure sites or structures were highly complementary. For obtaining a more precise identification of the discontinuity plans and movements, laser scanning showed to be the best option. The combination of both methods was quite opportune, in this case, because it allowed obtaining good documentation of the scenario while taking the most out of both approaches.

This study was funded by COMPETE2020 and FEDER funds in the scope of the GeoCrit project (POCI-01-0247-FEDER-047173).

References

1. J.H. Chandler, *The acquisition of spatial data from archival photographs and their application to geomorphology*, City University London (1989)
2. S.N. Lane, T.D. James, M.D. Crowell, Photogramm. Rec. **16** (2000)
3. N.J. Westoby, J. Brasington, N.F. Glasser, M.J. Hambrey, J.M. Reynolds, Geomorphology **179** (2012)
4. N.J. Rosser, D.N. Petley, M. Lim, S.A. Dunning, R.J. Allison, Q. J. Eng. Geol. Hydrogeol. **38** (2005)
5. J. Chandler, Earth Surf. Process. Landf. **24** (1999)
6. J. Lejot, C. Delacourt, H. Piégay, T. Fournier, M.-L. Trémélo, P. Allemand, Earth Surf. Process. Landf. **32** (2007)
7. C. Teixeira, A.C. Medeiros, Carta geológica de Portugal na escala 1:50 000 - Folha 5-C (Barcelos), (1969)
8. A.J. Riquelme, A. Abellán, R. Tomás, M., Jaboyedoff, Comput. Geosci. **68** (2014)